THE 3-D STUDY ON FLOW AROUND TWO WALL-MOUNTED CYLINDERS IN SIDE BY SIDE ARRANGEMENT

by

Tongxiao JIANG, Yuxiang YING, and Deming NIE*

Institute of Fluid Mechanics, China Jiliang University, Hanghzou, China

Original scientific paper
https://doi.org/10.2298/TSCI23S1039J

To investigate the characteristics of flow over two finite-height cylinders in side-by-side arrangement, 3-D numerical simulations are performed using the CFD technology for gap ratios (G = S/d, where d is the diameter of the cylinders, and S is the separation gap between the cylinders) between 1 and 4 at a Reynolds number of 100. The height-to-diameter ratio (h/d = 8, where h is the height of the cylinder) is fixed at 8. The drag and lift coefficients of the cylinders, as well as the Strouhal number are presented and compared with those of their 2-D counterparts. Our results show that the wake of the cylinders indicates a transition from the anti-phase state to the in-phase state at large gap ratios, accompanied by a decrease in the lift coefficients of the cylinders.

Key words: *adjacent, finite-height cylinder, wall-mounted, CFD, vortex*

Introduction

In fluid mechanics, the flow around multiple cylinders is an extremely important topic. When a cylinder is in the flow field, the vortex generated by the fluid-flow will exert a complex force on the cylinder, causing fatigue and damage to the cylinder. The flow around two parallel cylinders is one of the basic forms of flow around multiple cylinders; therefore, investigations into this type of flow are crucial and beneficial [1]. In the flow around multiple cylinders, the cylinders interfere with each other depending on the number, position, and gap of the cylinders, and the shape of vortex shedding differs differently from that of a single cylinder [2]. Currently, research pertaining to flow around double cylinders focuses on the effects of column arrangement, column gap ratio, and Reynolds number, on the flow field [3, 4]. Williamson [5] investigated the flow around two parallel cylinders under based on Re = 100 and 200, he discovered a coupling effect between the wake flow of the parallel cylinders, where synchronous in-phase and synchronous anti-phase states were indicated. Sumner *et al.* [6] conducted experiments on the flow around parallel double cylinders based on different Reynolds number (*i.e.*, Re = 500-3000) and different gap ratios, they successfully observed three different wake flow patterns. Wang and Lu [7] reported that the characteristics of the formation and shedding of a vortex street at the tail of a cylinder depends significantly on the gap ratio between cylinders, which has a critical value. Meanwhile, Zdravkovich *et al.* [8], Meneghini *et al.* [9], Cui [10], and Liu [11] showed that different flow phenomena appeared in flow fields with different gap ratios.

* Corresponding author, e-mail: nieinhz@cjlu.edu.cn

A review of the literature indicates sufficient research regarding 2-D flows around parallel cylinders. For example, Tong [12], Liu *et al.* [13], and Teng [14] investigated the flow field around two cylinders with different arrangements and gaps based on a 2-D flow. Investigations pertaining to the flow around 3-D finite-height double cylinders at low Reynolds number are scarce. Therefore, the flow around parallel finite-length double cylinders based on Re = 100 is investigated in this study, in addition the change in the wake flow by changing the gap ratio.

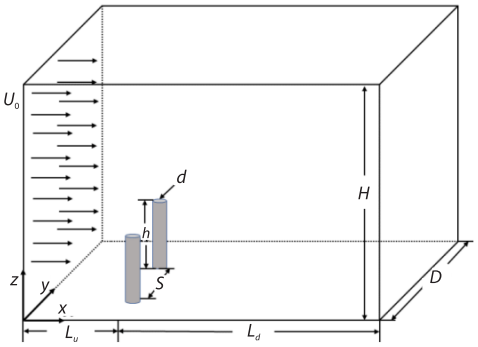

Figure 1. Model diagram

Problem description and numerical method

The computational domain as well as the size and location of the object for this study are shown in fig. 1. The computational domain measures $40d \times 30d \times 24d$. The distance between the finite-height cylinder and the entrance of the computational domain is $L_u = 12d$, and the distance from the exit of the computational domain is $L_d = 28d$. The diameter and height of the cylinder are denoted as d and h, respectively ($h/d = 8$ in this study), and the gap between the cylinders is denoted as S. In the calculation, d is set as 0.005 m.

In this study, the finite-length parallel double-cylinder flow is investigated based on $\mathrm{Re} = (U_0 d/\nu) = 100$, where ν is the kinematic viscosity of air, and the CFD technology is used to solve it. For the model shown in fig. 1, the following boundary conditions are imposed:

- Inlet: Velocity inlet, uniform flow rate of U_0.
- Outlet: Pressure outlet, relative pressure of 0.
- Symmetry: The front, back, and top surfaces are set as symmetry surfaces.
- Bottom: Wall, satisfying the no-slip boundary condition.
- Column surface: Wall, satisfying the boundary no-slip condition ($u = v = w = 0$) of the cylindrical surface velocity.
- Time step size: The appropriate step should be selected to satisfy the Courant-Friedrichs-Lewy condition [15]. In this study, the time step $\Delta t = 0.00137$ second.

To facilitate the comparison of fluid forces on the column, the lift and drag coefficients are introduced to describe the effect of the fluid on the column, and they are expressed:

$$C_l = \frac{F_l}{0.5\rho U_0^2 hd} \tag{1}$$

$$C_d = \frac{F_d}{0.5\rho U_0^2 hd} \tag{2}$$

where C_l is the lift coefficient, C_d – the drag coefficient, the lift force F_l is the force perpendicular to the direction of fluid-flow on the column, and the drag force F_d is the force parallel to the direction of fluid-flow.

The $St = (fd/U_0)$ represents the dimensionless vortex shedding frequency where f is the actual vortex shedding frequency.

Validation

In this study, the entire flow field is structurally meshed, and the computational domain is partitioned into seven regions, as shown in fig. 2. When the gap between the cylinders is sufficient, the $3d \times 3d$ region outside the cylinders is O-gridded. When the gap between the cyl-

inders is small, the O-gridded region is reduced based on the situation presented. The number of meshes in the cross-sectional area is increased, whereas those in the other areas are gradually reduced outward from the center of the column to increase the computational efficiency while maintaining computational accuracy

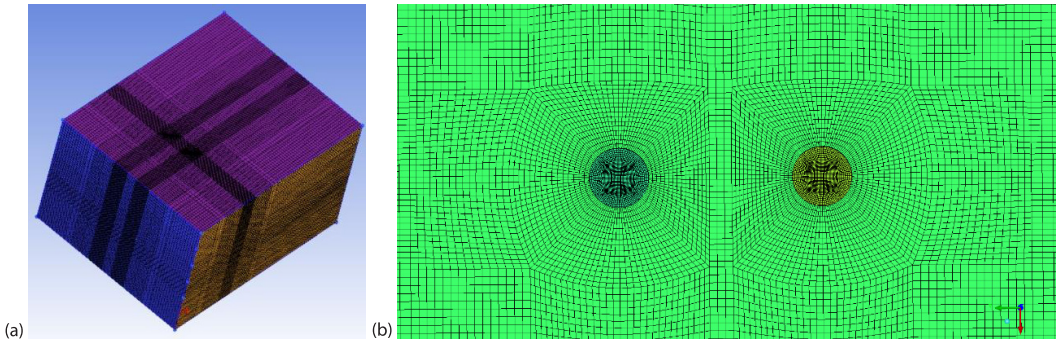

Figure 2. The 3-D grid of flow around two parallel cylinders (a) and parallel double cylindrical O-division area (b)

To verify the effect of the number of grids on the calculation accuracy, three sets of grids with different numbers of grids were selected for analysis and comparison. Because the computational accuracy of the numerical simulation should be improved as much as possible while ensuring the efficiency of the simulation, the number of grids was set to 4.6 million, as in Case 2 shown in tab. 1.

Table 1. Irrelevance verification of grids

Case	Number of grids	*St*
1	3.4 million	0.137453
2	4.6 million	0.137453
3	5.9 million	0.137453

To ensure the accuracy of the computational model, a physical model based on Re = 100 with a gap ratio $G = 0.5$ in the parallel double cylinders was used to perform a comparison in this study. In CFD simulation, the solution format is set to the SIMPLE format, the boundary second-order central difference is used, and the laminar model is selected for the solution calculation. For the same Reynolds number and the same boundary conditions, the time-averaged values of the lift coefficients of the cylinders were selected and compared with previous results. As shown by the results presented in tab. 2, the current simulation results are consistent with the previous results, and the errors are within the acceptable range, which verifies the accuracy of the computational model used in this study.

Table 2. Comparison of current results with results of previous studies

	$\bar{C}_{l1}$	Errors
[11]	0.471	1.9%
[2]	0.475	2.8%
Current study	0.462	–

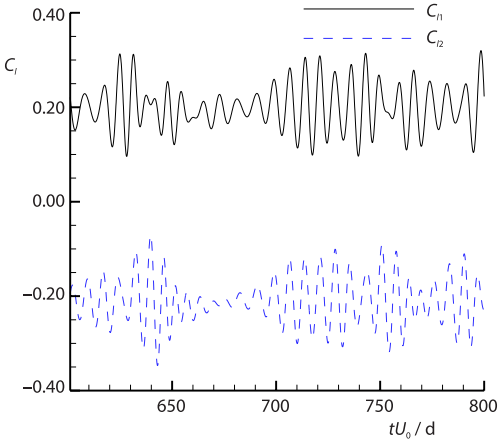

Figure 3. Time history of lift coefficients for both cylinders at $G = 1$

Numerical results

This paper focuses on the variation in an entire flow field for a gap ratio G between 1.0 and 4.0. The wake flow of the two cylinders show a non-periodic variation when G is less than 2.4. As shown in fig. 3, when G is less than 2.4, the lift curve of the cylinder is a sine curve with an unstable amplitude. Furthermore, the forces on the two cylinders are simultaneously inconsistent, but the magnitudes of the average lift coefficients of the cylinders are approximately equal. When viewed in general, the curve shows certain regularity over a long period. As shown in fig. 4, the vortex exhibits a synchronous in-phase when it first sheds from the cylinder at G = 1.0. Meanwhile, the structure of the flow field in fig. 4 shows that when G is not sufficiently large, the wake flow of the two cylinders intersects, thereby hindering independent vortex shedding.

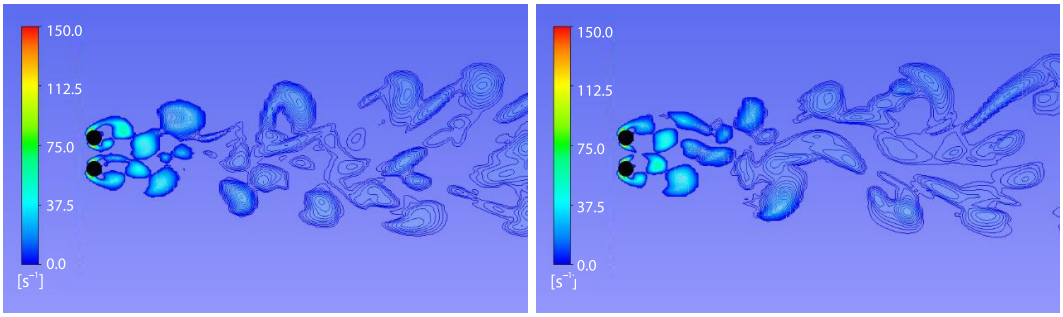

Figure 4. Vorticity diagram of flow field at $G = 1$

When G is larger than 2.4, the variation in the wake flow of the cylinder changes from non-periodic to periodic. As shown in fig. 5, the cylindrical lift coefficient curve at G = 2.8 is a sinusoidal curve with a stable amplitude, therefore, G = 2.4 can be regarded as the critical gap ratio at which the wake flow pattern changes. According to Lin *et al.* [2], G = 1.2 is the critical gap ratio at which the wake flow varies periodically in a 2-D simulation. Compared with the 2-D flow, the 3-D flow around the cylinder required a larger gap to exhibit periodic changes in the wake.

When G exceeds 2.4, the flow field presents two different stable states, as shown in figs. 5(b) and 6. First, the synchronous anti-phase state is stable for a certain duration, subsequently, it changes to the synchronous in-phase state. As shown in fig. 6(a), the lift forces on the two cylinders are equal in magnitude and opposite in direction, which is the synchronous anti-phase state of the flow field. Figure 6(b) shows that the cylindrical lift curves are in the same phase at this time, which is known as the synchronous and in-phase states. In addition, the amplitude of the lift force when the cylinder is in the synchronous anti-phase is greater than that when it is in the synchronous in-phase, the details of which will be provided later.

To visualize the characteristics of the flow field in two different states more clearly, an analysis was performed based on four representative moments of complete vortex shedding in

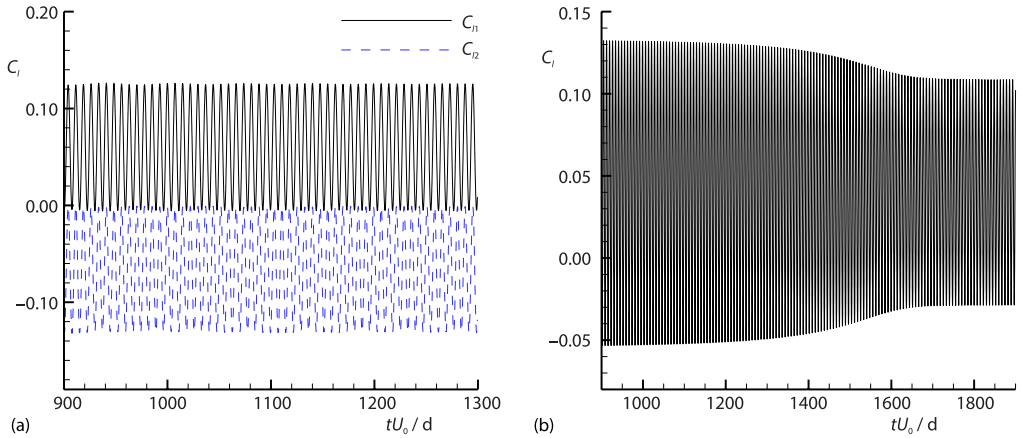

Figure 5. Time history of lift coefficient of both cylinders at $G = 2.8$ (a) and time history of lift coefficient of cylinder 1 at $G = 4.0$ (b)

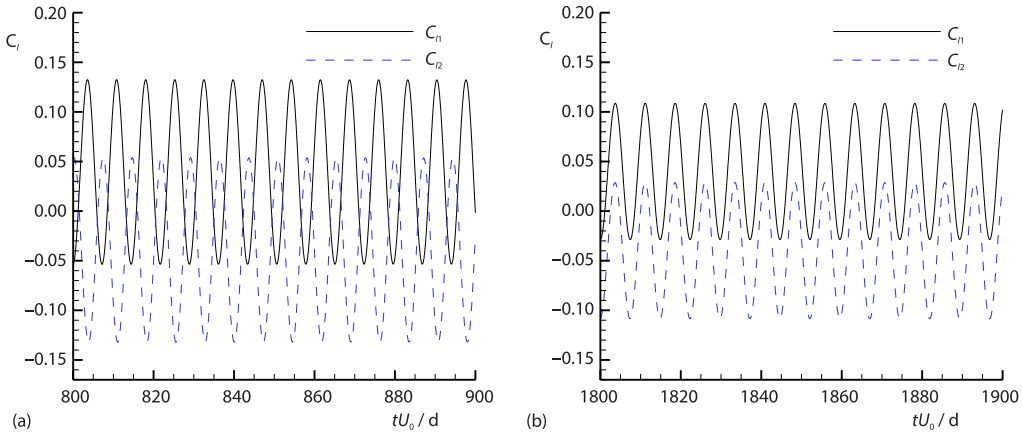

Figure 6. Time history of partial lift coefficient at $G = 4.0$

two states. The four moments are $t = 0$, $t = T/4$, $t = T/2$, and $t = 3T/4$, where T is the dimensionless period of vortex shedding and is expressed as $T = 1/St$.

The 3-D vorticity diagrams and top views of the vorticity at $z = h/2$ at different moments are shown in four plots in figs. 7 and 8, respectively. These figures show that the cylindrical wake flow has completed a complete vortex shedding cycle in the synchronous and in-phase modes.

Figures 9 and 10 show 3-D vorticity diagrams and a top view of the vorticity of the flow field at $z = h/2$ at four different moments, respectively. It shows that the synchronous anti-phase vortex shedding mode completes one cycle.

It is noteworthy that the generation of the vortex street around the cylinder is due to the pressure difference on both sides of the cylinder. As shown in the previous figures, when the flow field is in the synchronous anti-phase state, two large vortices or two small vortices appear in the middle of the flow field, whereas when the flow field is in the synchronous homogeneous state, a large vortex and a small vortex appear in the middle of the flow field. Therefore, when the flow field is in the synchronous anti-phase state, the pressure difference on both sides of the

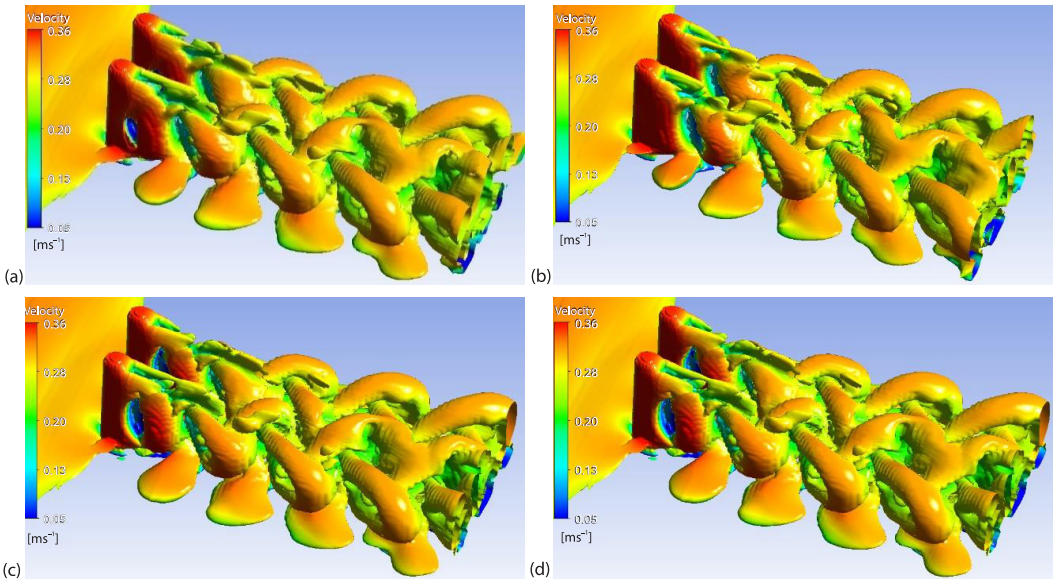

Figure 7. The 3-D vorticity diagrams at different moments in synchronous in-phase state at $G = 4.0$; (a) $t = 0$, (b) $t = T/4$, (c) $t = T/2$, and (d) $t = 3T/4$

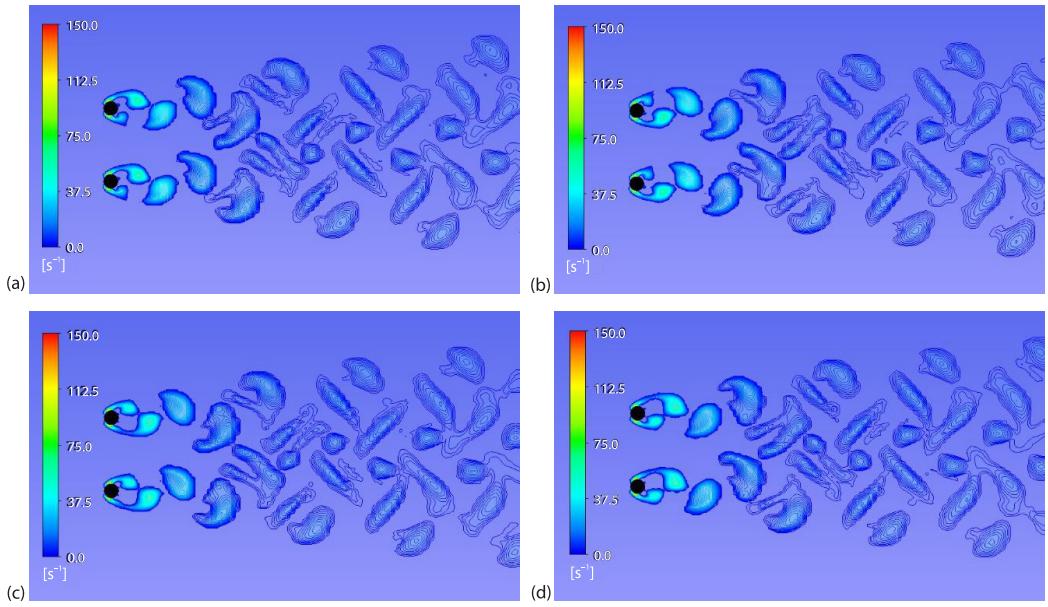

Figure 8. Vorticity diagrams of different moments in synchronous in-phase state at $G = 4.0$; (a) $t = 0$, (b) $t = T/4$, (c) $t = T/2$, and (d) $t = 3T/4$

cylinder will be greater than that in the synchronous in-phase state, therefore, the amplitude of the lift force on the cylinder in the synchronous anti-phase state will be greater than that on the cylinder in the synchronous in-phase state.

As previously mentioned, the pressure difference between the two sides of the cylinder when the anti-phase state is maintained will be greater than that between the two sides of the

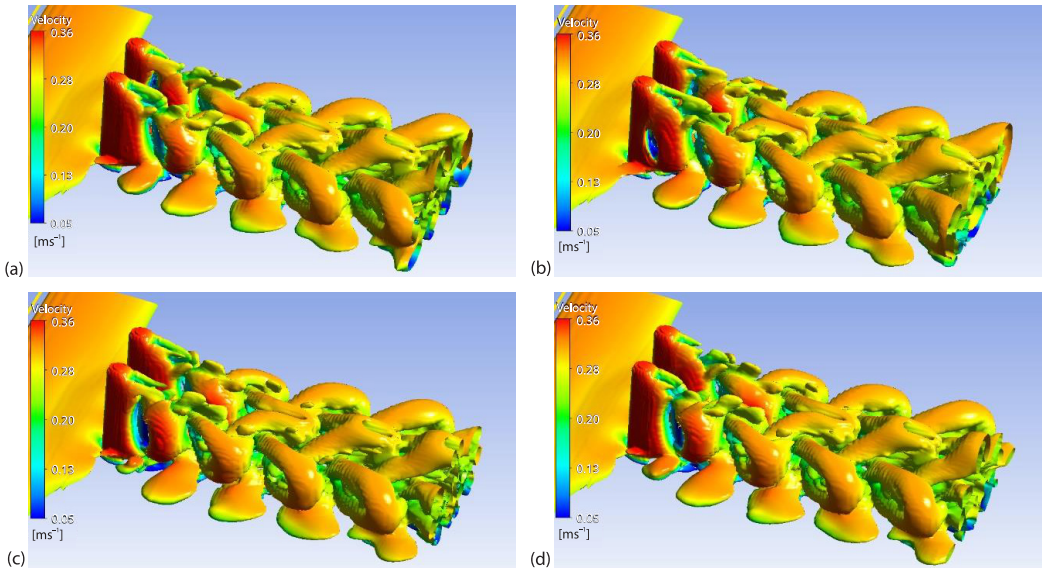

Figure 9. The 3-D vorticity diagrams at different moments in synchronous anti-phase state at $G = 4.0$; (a) $t = 0$, (b) $t = T/4$, (c) $t = T/2$, and (d) $t = 3T/4$

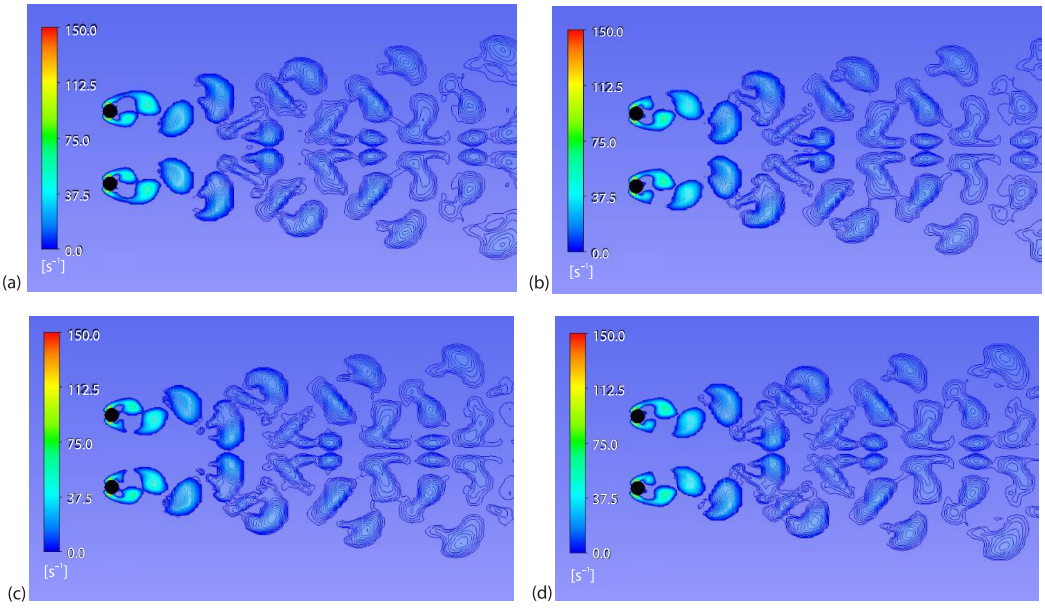

Figure 10. Vorticity diagrams of different moments in synchronous anti-phase state at $G = 4.0$; (a) $t = 0$, (b) $t = T/4$, (c) $t = T/2$, and (d) $t = 3T/4$

cylinder when the in-phase state is maintained, therefore, after a certain duration, the flow field will change to the synchronous in-phase state, where the pressure difference is less significant. As such, the flow field does not remain stable in the synchronous anti-phase state but changes to the synchronous in-phase state.

Figures 11 shows the 3-D and 2-D simulation results, respectively. As shown, the average drag coefficient of both decreases as the gap increases. The drag coefficients of the two cylinders in both the 2-D and 3-D simulations remain the same. The average drag coefficient of the 3-D simulation is smaller than that of the 2-D simulation because of the suppression effect of the free end. Figure 11(b) shows that the average lift coefficients of the two cylinders for the same gap in 2- and 3-D are equal in magnitude and opposite in direction. As the gap increases, the average lift coefficient approaches zero. Similarly, the average lift coefficient of the 3-D simulation is smaller than that of the 2-D simulation for the same gap ratio.

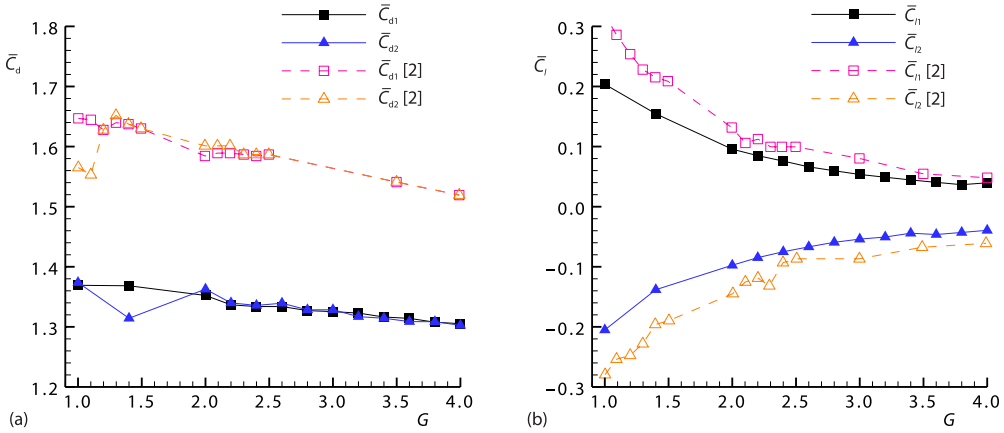

Figure 11. The $\bar{C}_d$ *vs.* G (a) and $\bar{C}_l$ *vs.* G (b)

As shown in fig. 12(a), when G exceeds 2.4, the amplitudes of the lift coefficients of the two states for the same gap are different, and the amplitude of the lift coefficient of the synchronous anti-phase state is greater than that of the synchronous in-phase state. As the gap ratio increases, the amplitude of the lift coefficient of the cylinder in the synchronous anti-phase state decreases whereas that in the synchronous in-phase state increases. The amplitude of both will likely be the same value after the gap ratio increases to a certain number. The Strouhal number stabilizes at approximately 0.18 after the flow field shows periodic changes during the 2-D simulation [2]. As shown in fig. 12(b), the Strouhal number in this study is smaller than that in

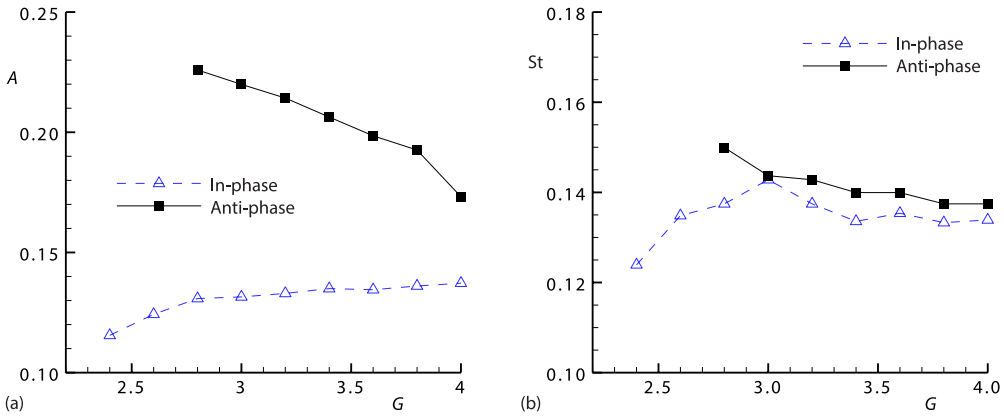

Figure 12. Amplitude of lift coefficient as a function of gap for different states (a) and Strouhal number as a function of gap for different states (b)

the 2-D simulation. Figure 12(b) shows the trend of Strouhal number in the two states as function of the gap ratio between the cylinders, as the gap ratio increases, the Strouhal number in the synchronous anti-phase state decreases and finally remains stable. Meanwhile, the Strouhal number in the synchronous in-phase state increases with the gap and finally stabilizes.

Conclusions

This study simulated and investigated the flow around parallel double cylinders with a limited height under Re = 100. The changes in the force and flow field of the cylinder at gap ratios of 1.0 and 4.0 were focused on, and the following conclusions are as follows.

- When Re = 100 and the G of the flow around the finite-length parallel double cylinders was less than 2.4, the vortex street generated by the two cylinders intersected, whereas the entire flow field indicated non-periodic changes. When G exceeded 2.4, the vortex streets generated by the cylinders did not intersect, and the flow field exhibited periodic changes. In fact, $G = 2.4$ can be considered the critical gap ratio for the transition of the flow field properties. The vortex street generated by the cylinder showed a periodic change, *i.e.*, it maintained a synchronous anti-phase state for certain duration and then changed to a synchronous in-phase state.
- The average lift coefficient and average drag coefficient of the 3-D flow around the cylinder exhibited the same characteristics and trends as those of the 2-D simulation but were smaller quantitatively.
- The magnitudes of the lift coefficient and Strouhal number when the cylinder was in the synchronous anti-phase were greater than those when the cylinder was in the synchronous in-phase for the same gap. The amplitude of the lift coefficient in the synchronous anti-phase state decreased as the gap ratio increased, whereas that in the synchronous in-phase state increased with the gap ratio. The Strouhal number in the synchronous anti-phase state decreased as the gap ratio increased and then stabilized, whereas the Strouhal number in the synchronous in-phase state increased with the gap ratio and then stabilized. The value of Strouhal number in the two states was approximately equal when the gap was sufficiently large.

Acknowledgment

This study was supported by the National Natural Science Foundation of China (Nos. 12132015 and 11972336).

References

[1] Li, Y., *et al.*, The 3-D Numerical Simulation of Flow around Two Side-by-Side Circular Cylinders at High Reynolds Numbers Using DES Method (in Chinese), *Journal of Hydrodynamics*, *29* (2014), 4, pp. 412-420
[2] Lin, L., *et al*., Numerical Simulation of the Characteristics and Interaction of Flow around Side-by-Side Arranged Circular Cylinders (in Chinese), *Chinese Journal of Applied Mechanics*, *38* (2021), 2, pp. 844-850
[3] Sumner, D., Two Circular Cylinders in Cross-Flow: A Review, *Journal of Fluids and Structures*, *26* (2010), 6, pp. 849-899
[4] Cui, W., *et al*., Study on Influence Factors of Flow around Twin Tandem-Circular Cylinders under High Reynolds Number (in Chinese), *Water Resources and Hydro power Engineering*, *49* (2018), 2, pp. 92-98
[5] Williamson, C., Evolution of a Single Wake behind a Pair of Bluff Bodies, *Journal of Fluid Mechanics*, *159* (1985), 1, pp. 1-18
[6] Sumner, D., *et al*., Fluid Behavior of Side-by-Side Circular Cylinders in Steady Cross-Flow, *Journal of Fluids and Structures*, *13* (1999), 3, pp. 309-338
[7] Wang, Y., Lu, L., Numerical Simulation of Flow around Multi-Circular Cylinder (in Chinese), *Journal of Chongqing University of Technology*, *30* (2016), 2, pp 37-40

[8] Zdravkovich, M., Thr Review of Flow Interference between Two Circular Cylinders in Various Arrangements, *Journal of Fluids Engineering*, *99* (1977), 4, pp. 618-633
[9] Meneghini, J., *et al*., Numerical Simulation of Flow Interference between Two Circular Cylinders in Tandem and Side-by-Side Arrangements, *Journal of Fluids and Structures*, *15* (2001), 2, pp. 327-350
[10] Cui, X., Hydrodynamic Characteristics of Flow around Two Parallel Cylinders (in Chinese), M. D. thesis, China Ocean University, Qingdao, China, 2014
[11] Liu, S., Numerical Investigation on Vortex-Induced Vibrations of Two Side-by-Side Arranged Circular Cylinders at a Low Reynolds Number (in Chinese), M. D. thesis, Tianjin University, Tianjin, China, 2014
[12] Tong, X., Numerical Simulation Research on Flow Characteristics of Flow around Cylinder under Low Reynolds Number Based on FLUENT (in Chinese), M. D. thesis, Yangzhou University, Yangzhou, China, 2021
[13] Liu, X., *et al*., A Numerical Study on Resistance Characteristics of Flow around Two Cylinders (in Chinese), *Chinese Journal of Theoretical and Applied Mechanics*, *41* (2009), 3, pp. 300-306
[14] Teng, L., Simulation of Flow around Two Cylinders under Different Arrangement, *Water Science and Engineering Technology*, *4* (2016) (in Chinese), pp. 39-41
[15] Wang, X., *et al*., Numerical Simulation of 3-D Flow around a Circular Cylinder of Finite Length (in Chinese), *Chinese Journal of Ship Research*, *13* (2018), 2, pp. 27-34

Paper submitted: February 12, 2022
Paper revised: March 4, 2022
Paper accepted: March 14, 2022